HHS Public Access

Author manuscript

J Mol Cell Cardiol. Author manuscript; available in PMC 2016 July 01.

Published in final edited form as:

J Mol Cell Cardiol. 2015 July ; 84: 1–9. doi:10.1016/j.yjmcc.2015.03.012.

Cardiac Myocyte Alternans in Intact Heart: Influence of Cell-Cell Coupling and β-Adrenergic Stimulation

Karin P. Hammer[a,1], **Senka Ljubojevic**[b], **Crystal M. Ripplinger**[a], **Burkert M. Pieske**[b,c], and **Donald M. Bers**[a]

Karin P. Hammer: karin.hammer@ukr.de; Senka Ljubojevic: lj.senka@gmail.com; Crystal M. Ripplinger: cripplinger@ucdavis.edu; Burkert M. Pieske: burkert.pieske@medunigraz.at; Donald M. Bers: dmbers@ucdaivs.edu

[a]Department of Pharmacology, University of California, Davis, GBSF, Davis, CA 95616-8636, USA

[b]Department of Cardiology, Medical University of Graz, Auenbruggerplatz 15, 8010 Graz, Austria

[c]Department of Cardiology, Charité - Medical University Berlin, Augustenburgerplatz 1, 13353 Berlin, Germany

Abstract

Background—Cardiac alternans are proarrhythmic and mechanistically link cardiac mechanical dysfunction and sudden cardiac death. Beat-to-beat alternans occur when beats with large Ca^{2+} transients and long action potential duration (APD) alternate with the converse. APD alternans are typically driven by Ca^{2+} alternans and sarcoplasmic reticulum (SR) Ca^{2+} release alternans. But the effect of intercellular communication via gap junctions (GJ) on alternans in intact heart remains unknown.

Objective—We assessed the effects of cell-to-cell coupling on local alternans in intact Langendorff-perfused mouse hearts, measuring single myocyte [Ca^{2+}] alternans synchronization among neighboring cells, and effects of β-adrenergic receptor (β-AR) activation and reduced GJ coupling.

Methods and Results—Mouse hearts (C57BL/6) were retrogradely perfused and loaded with Fluo-8 AM to record cardiac myocyte [Ca^{2+}] in situ with confocal microscopy. Single cell resolution allowed analysis of alternans within the intact organ during alternans induction. Carbenoxolone (25 μM), a GJ inhibitor, significantly increased the occurrence and amplitude of alternans in single cells within the intact heart. Alternans were concordant between neighboring cells throughout the field of view, except transiently during onset. β-AR stimulation only reduced Ca^{2+} alternans in tissue that had reduced GJ coupling, matching effects seen in isolated myocytes.

Corresponding author: Dr. Donald M. Bers, Ph.D., Department of Pharmacology, University of California, Davis, Genome Building 3511, Davis, CA 95616-8636, Ph: 530-752-6517, FAX: 530-752-7710, dmbers@ucdavis.edu.

[1]present address: Department of Internal Medicine II, University Hospital Regensburg, Franz-Josef-Strauss-Allee 11, 93053 Regensburg, Germany; karin.hammer@ukr.de

Disclosures

None declared.

Conclusions—Ca^{2+} alternans among neighboring myocytes is predominantly concordant, likely because of electrical coupling between cells. Consistent with this, partial GJ uncoupling increased propensity and amplitude of Ca^{2+} alternans, and made them more sensitive to reversal by β-AR activation, as in isolated myocytes. Electrical coupling between myocytes may thus limit the alternans initiation, but also allow alternans to be more stable once established.

Keywords

Calcium; whole heart; alternans; β-adrenergic receptor activation

1. Introduction

Cardiac Ca^{2+} alternans is defined as a beat-to-beat alternation in Ca^{2+} transient (CaT) amplitude and is tightly connected with mechanical and electrical alternans. Cardiac alternans has been shown to be Ca^{2+} driven [1, 2] and CaT alternans can occur without action potential duration (APD) alternans, [3, 4] but the two can influence each other [5, 6]. Ca^{2+} alternans can be seen within regions of a myocyte [7, 8] as well as myocyte-wide alternans and both regional and whole heart alternans. Clinically, T-wave alternans (TWA) is an important marker for the risk of ventricular arrhythmia and is associated with Ca^{2+} and APD alternans [9, 10], and small changes in Ca^{2+} cycling can cause reentrant arrhythmias [11]. In disease models, CaT alternans can be observed long before arrhythmias or heart failure occurs [12]. Hence, TWA and Ca^{2+} alternans can be an index of propensity for arrhythmias and pharmacological interventions [13]. Alternans is found in numerous disease conditions (e.g. ischemia, heart failure and acidosis) as a prominent arrhythmogenic factor linked to cardiac fibrillation in humans and as a precursor of heart failure [14].

CaT alternans involves several aspects of excitation-contraction-coupling (ECC) and SR Ca^{2+} release. Changes in SR load often occur during Ca^{2+} alternans, but the initiation of alternans seems likely to encroach on ryanodine receptor (RyR) refractoriness or availability [2, 15]. Indeed, Ca^{2+} sparks and global CaT depend not only on the rate of refilling but also on RyR refractoriness [16, 17]. As pacing rate increases, RyR refractoriness seems to be the first factor to initiate alternans and it can cause both SR Ca^{2+} load and APD alternans at higher rates [18].

Cellular mechanisms of cardiac alternans are well studied. However, it is less clear how this is influenced in the intact heart by intercellular communication, where Ca^{2+} induced APD alternans can disperse into the surrounding tissue [17]. This voltage spread via gap junctions (GJ) may help synchronize subcellular Ca^{2+} release patterns as well as spatially discordant Ca^{2+} alternans [19, 20]. GJs may help to maintain Ca^{2+} homeostasis in coupled myocytes and partial uncoupling can induce severe arrhythmias [21, 22]. However, it is unknown how partial GJ uncoupling affects myocyte Ca^{2+} alternans in intact heart, and whether neighboring myocytes exhibit synchronized alternans phase.

The β-AR agonist isoproterenol (ISO) exerts inotropic effects due, in part to accelerated SR Ca^{2+} uptake and release [23, 24] and enhancement of L-type Ca^{2+} current [25]. The faster SR Ca^{2+} uptake accelerates SR Ca^{2+} refilling and relaxation (lusitropy). Indeed, β-AR stimulation can curtail cardiac alternans due to its effects on Ca^{2+} transient kinetics in both

ventricular [3] and atrial myocytes [26]. However, it is less clear how this translates to the whole heart where intercellular communication influences Ca^{2+} cycling and ECC.

The present study aimed to test the hypothesis that frequency induced myocyte CaT alternans in intact mouse heart is influenced by ISO and intercellular communication. We used confocal microscopy of Langendorff-perfused mouse hearts, allowing analysis of subcellular Ca^{2+} cycling within the intact heart to elucidate how mechanisms found in isolated myocytes translate to the organ level. Specifically we sought to evaluate the role of GJ coupling during alternans and the effects of β-AR stimulation on cardiac alternans on the tissue scale.

2. Material and Methods

2.1. Animals

All animal procedures were approved by the Animal Care and Use Committee of the University of California, Davis and adhered to the NIH Guide for the Care and Use of Laboratory Animals. Adult male C57BL/6 mice (10–20 weeks) were anesthetized with Isoflurane/oxygen mix (95/5). Hearts were quickly excised, cannulated and Langendorff perfused at 37°C in normal Tyrode's solution (NT: NaCl 135 mM; KCl 5.4 mM; $CaCl_2$ 2mM; $MgCl_2$ 1 mM; Glucose 10 mM; Hepes 10 mM; pH 7.35, adjusted with NaOH). Intrinsic heart rate was slowed to 2–4 Hz) by removing the SA-node and crushing the AV-node. Hearts were electrically paced at the base, via two Ag/AgCl electrodes at the ventricular base (far from the confocal imaging site), via square pulses (5Hz or basic cycle length, BCL 200 ms) unless noted otherwise. The stimulation frequency was always faster than the remaining intrinsic heart rate after partial destruction of the AV-node.

To isolate myocytes for single cell studies, mouse hearts were perfused with a liberase-based Langendorff perfusion protocol as described previously [27].

2.2. Confocal Microscopy

After hearts displayed regular, albeit slowed heart rate, they were loaded at room temperature (RT) with Fluo8-AM (AAT bioquest, Inc., Sunnyvale, CA; 3.75 μM) and Di-4-ANEPPS (Biotium, Inc., Hayward, CA; 5 μM) for fluorescent imaging of intracellular Ca^{2+} and V_m, respectively. To eliminate motion artifacts, blebbistatin (Abcam Biochemicals, Cambridge, MA; 10–20 μM) was added to the perfusion solution during recording. Fluorescence from 8 to 16 neighboring cells was recorded using a confocal microscope (FluoView™ FV1000, Olympus America Inc., Center Valley, PA) in *x-y* or line scan mode with a sampling speed of 2.1 ms per line. Experiments were performed using a 20× air objective. Argon laser excited (480 nm) fluorescence and emission was collected with a 510 long pass filter for Fluo8 or two band pass filters (500–550 nm and 600–700 nm) if Fluo8 was measured simultaneously with Di-4-ANEPPS. Excitation intensity and exposure times were kept as short as possible (≤20 s for a given region) to assure reasonable signal-to-noise values, stability of steady state Ca^{2+} transients and limited phototoxicity. Since Di-4-ANEPPS has a ~10-fold lower fractional fluorescence change compared to Ca^{2+} indicators, the signal-to-noise ratio in voltage signals at the single myocyte level are expected to be lower.

For single myocyte experiments, cells were loaded with Fluo-4 (Molecular Probes, Leiden, The Netherlands) as described previously [27] and placed on the stage of an inverted microscope equipped with a 40×/1.3 N.A. oil-immersion objective and a Zeiss LSM 510 Meta confocal laser point scanning system (Zeiss, Jena, Germany) or an Olympus Fluoview™ 1000 confocal microscope (Olympus, Center Valley, PA, USA). Excitation and emission wavelengths were 488 and >515 nm, respectively. Cells were field-stimulated via platinum electrodes.

2.3. Temperature

Experiments were performed at RT (22–25°C). Alternans is temperature dependent and at lower temperature the frequency needed to evoke Ca^{2+} alternans changes, but it does not change the alternans pattern [3, 28, 29]. RT allows applying less stressful, but longer protocols and thereby more reliable information can be collected from the hearts. Furthermore indicator retention by the myocytes is greatly improved at RT vs. 37°C.

2.4. β-AR and electrical stimulation and GJ uncoupling

The β-AR agonist isoproterenol (ISO; Sigma-Aldrich, St. Louis, MO; 10 μM) and partial GJ-uncoupler Carbenoxolone (CBX; Sigma-Aldrich, St. Louis, MO; 25 μM) was delivered by global perfusion. For single cell experiments the delivery of the β-AR agonist isoproterenol was achieved by bath perfusion and thus could be reduced to 30 nM

2.5. Data Analysis

Data analysis was performed with ImageJ (NIH, Bethesda, MD) for image analysis and IgorPro (WaveMetrics Inc., Lake Oswego, OR) for Ca^{2+} transient analysis. To quantify alternans amplitude, an alternans ratio r was calculated ($r = 1 – S/L$) where S and L are amplitudes of the small and large transient [8, 30]. Resulting ratios are between 0 and 1, where 0 indicates no alternans and 1 is where every other AP fails to activate a Ca^{2+} transient. Cells with $r > 0.08$ were considered alternating (i.e. exceeding noise levels in the recordings).

Statistics were calculated with GraphPad Prism (GraphPad Software, Inc., La Jolla, CA). Comparisons between two groups of data were made using Student's t-test and multiple comparisons were made using one- or two-way analysis of variance (ANOVA) with Dunn's post-hoc-testing. $P<0.05$ was considered statistically significant.

3. Results

3.1. Measuring $[Ca^{2+}]_i$ in intact mouse heart with confocal microscopy

The left ventricular epicardium of Fluo8-loaded heart was put into focus on a laser scanning confocal microscope. For 2-dimensional images (Fig 1A), the area is scanned line by line, starting from the upper left corner. The time to record a single pixel on that line was 2 μs, and a complete line 2.1 ms, so the whole frame was recorded in 1.1 s. During this time four Ca^{2+} transients are visible as bright lines of fluorescence intensity across all cells in the field of view. For line scans, the line was always positioned perpendicular to the long axis of the cells. This ensures visualization of many myocytes during each 2 ms line scan, providing

high temporal resolution (Fig 1B). All cells within the field of view are expected to be activated simultaneously independent of the orientation. That is, even for transverse propagation velocity in mouse (340 mm/s [31]), all myocytes would be activated in ≤1 ms. Along this line the scan (2 ms per line), individual Ca^{2+} signals from all twelve myocytes are obtained for further analysis (Fig 1B).

3.2. Pacing-induced Ca^{2+} alternans in intact hearts

Pacing frequency was progressively increased from 5 to 10 Hz (1 Hz increments) and the BCL at which stable Ca^{2+} alternans was assessed. Under control conditions (NT) at 5 Hz 11.6% of the cells exhibited Ca^{2+} alternans, but 100% of cells displayed alternans at 7Hz stimulation (Fig 2A). Hearts not electrically stimulated had intrinsic rates between 2 to 4Hz, most likely due to residual activity of the AV-node or HIS bundle region of the hearts.

At 5 Hz steady state pacing, addition of ISO had no effect on alternans (Fig 2B; 11.6 ±6.6% of control cells vs. 15.2 ±2.8% after β-AR). This contrasts with reports from single mouse myocytes, where β-AR can reduce or abolish alternans (see myocyte studies below). This suggests an influential role of intercellular communication on the maintenance of Ca^{2+} cycling and alternans within cardiac myocytes in situ.

Alternans amplitude was observed with r ranging from 0 to 1. We found different patterns of alternans that are illustrated by two examples depicted in Fig 2C. Some cells had an apparent 2:1 pattern in their CaT alternans (r=1) but often a small, transient Ca^{2+} increase (or inflection) was visible in the $[Ca^{2+}]_i$ decay, consistent with an AP-induced small Ca^{2+} increase during that phase. Fig 2D shows representative CaT with alternans ratios from 0 to 1, where the asterisks indicate the electrical stimulus. The timing (and spatial synchrony) of the small transient $[Ca^{2+}]_i$ increase in trace with ratio 0.8 indicates that this is due to the electrical stimulus. To verify that these events were indeed attributable to APs (not afterdepolarizations or excitation failures), especially for cells with r=1 (2:1) alternans, we tested for the presence of APs. We simultaneously recorded Ca^{2+} and membrane voltage (V_m) with Di-4-ANEPPS in addition to Fluo-8 in five hearts. Fig 2E shows a representative 2-dimensional snapshot of cardiac tissue with double staining (red is Di-4-ANEPPS and green is Fluo-8). The V_m traces in double-stained tissue confirmed that at least up to 7 Hz, every stimulus led to a voltage signal, even when Ca^{2+} transients were only apparent at alternate stimuli.

3.3. Reduced GJ coupling alters the incidence and amplitude of CaT alternans

As we found that intercellular communication may influence Ca^{2+} cycling in myocytes within the intact heart, we tested whether partial uncoupling with CBX has any effect on CaT kinetics. The CaT in cells from normally coupled tissue had a shorter time to peak compared to cells with reduced GJ coupling (25.3 ±0.6 vs 31.5 ±1.9 ms) while the decay time was unaltered by GJ inhibition by CBX (144 ±13.5 ms vs 155 ±20.7 ms in CBX, Fig 3A) even with β-AR stimulation (94.5 ±7.2 ms vs 99.2 ±12.0 ms in CBX, Fig 3A). Upon reduction of coupling efficacy the electrical signal can less easily be spread among neighboring cells which may slightly alter the rate of rise of the APs. That would slow the time to peak values of the Ca^{2+} transients. Consistent with this, we previously showed that

25 μM CBX slowed conduction velocity by 25% in rabbit hearts , and in pilot experiments in mouse this reduction was 16–20% (not shown). In our hands, all Ca^{2+} transients within the field of view were initiated at the same time (Fig 3B). Reduced GJ coupling also affected the incidence and ratio of CaT alternans at 5 Hz (Fig 3C). A much higher number of cells displayed alternans in partially uncoupled tissue (81.5 ±13.8% vs. 11.6 ±6.6%) and the alternans ratio was also much higher (0.47 ±0.04 0.17 ±0.03), indicating that electrical coupling between cells in the heart limits alternans in the myocytes. Partial uncoupling may make the cells behave more like isolated myocytes with respect to alternans induction, so we also examined isolated myocytes.

3.4. β-AR stimulation inhibits alternans induced by GJ uncoupling

Single myocyte experiments have shown that β-AR stimulation has inhibitory effects on the occurrence and intensity of Ca^{2+} alternans [3, 26]. We tested whether β-AR stimulation would curtail myocyte alternans in intact tissue more effectively when GJs are partially uncoupled. While reduction of alternans incidence with β-AR was not significant (68.8 ±22.5% under ISO vs. 81.5 ±13.8% in control; Fig 4A), there was a 50% reduction in alternans amplitude observed (r was reduced from 0.47 ±0.04 to 0.23 ±0.03; Fig. 4A) similar to the value in normally coupled tissue with ISO (0.21 ±0.03; Fig 2B).

To test whether totally uncoupled myocytes from our mouse hearts would show β-AR reduction of alternans, we studied effects of ISO on isolated mouse ventricular myocytes stimulated at 5 Hz at RT. ISO completely abolished the alternans ratio in isolated cells (Fig 4B–C). The alternans ratios found in single cells were comparable to those found in cells within the intact tissue (0.22 ±0.14; Fig 2B) and these values also translated into contractile alternans of the isolated cells (0.19 ±0.04). The observed contraction alternans was also abolished by the application of ISO.

3.5. Transition to stable alternans depends on GJ coupling

During steady state stimulation we found that all cells within a field of view were spatially concordant and displayed stable alternans at 7 Hz (Fig 2A). Here we sought to evaluate how cells transition into alternans upon a change in BCL within intact tissue. We switched stimulation frequency from 5 to 7 Hz and measured $[Ca^{2+}]_i$ in the myocytes.

We expected that the sudden shortening of the diastolic interval would set the phase of alternans in all cells equally, since the first CaT after frequency increase would have less SR Ca^{2+} and RyR available for release (favoring a small beat). Indeed, the first beat was smaller in amplitude, but alternans was not immediately induced. A brief compensated state of Ca^{2+} cycling was characterized by non-alternating, albeit smaller, CaT amplitudes (Fig 5A). That was followed by a decompensated state during which the alternans developed, and CaT amplitude of the large transients increased and the smaller transients decreased (Fig. 5A). In cases where Ca^{2+} alternans already occurred at 5 Hz a comparable pattern was observed (Fig 5B). Upon frequency increase, alternans ratio was maintained or slightly reduced with overall smaller CaT amplitudes during the compensated state, followed by a decompensated state with increased alternans ratio (more than 0.1 increase compared to the initial ratio) and larger CaT amplitude of the large transients (Fig 5B). The duration of the compensated

phase of Ca^{2+} cycling was not affected by β-AR stimulation (1.4 ± 0.1 s vs. 1.2 ± 0.2 s) but CBX significantly decreased the compensated phase with or without ISO (0.5 ± 0.2 s vs 0.5 ± 0.05 s, Fig. 5C).

In a subset of measurements, GJ uncoupling led to a severely decompensated Ca^{2+} handling after frequency increase. In these cases, tissue displayed no CaT's, only spontaneous Ca^{2+} release in form of Ca^{2+} waves. These waves were not synchronized among neighboring cells nor did they cross the cell borders. Reducing stimulation frequency restored normal Ca^{2+} cycling (Fig 5D).

3.6. Spatially discordant alternans occurs transiently upon β-AR stimulation

In all of our experiments neighboring cells exhibited spatially synchronized alternans phase among neighbors during steady state pacing, and spatially discordant alternans was not observed. This raised the following question. If alternans phase was not locked uniformly by the initial shortened diastolic interval (compensated phase), do individual cells start alternans phase randomly with respect to their neighbors? Only during β-AR stimulation did we see a subset of cells that transiently displayed spatially discordant alternans during the early stage of alternans (Fig 6). However, even in these cases spatial concordance was restored over the course of just a few beats, typically over the course of 2 to 3 transients. The eventually dominant cells seem to shorten the small CaT duration and quash the large CaT (asterisks in Fig 6C, right), until synchronization was reached and all cells displayed concordant alternans.

Upon frequency increase, all of the control cells were concordant with their neighbors and only 17% of the ISO treated cells were discordant with respect to their neighbors (Fig 6E). In this case GJ coupling did not seem to matter (18% with ISO and CBX). Thus, ISO and the acceleration of $[Ca^{2+}]_i$ decline and SR Ca restitution may have been critical to the appearance of spatial discordance, while cell-cell coupling (even with CBX) was sufficient to strongly drive spatial concordance.

4. Discussion

In the present study we analyzed pacing-induced CaT alternans in intact mouse hearts. We found that frequency-induced alternans is spatially concordant among neighboring epicardial, left-ventricular myocytes. Partial GJ uncoupling increased the amplitude of Ca^{2+} alternans, but did not alter local concordance among neighboring cells. This emphasizes that alternans as a proarrhythmic factor would be enhanced in disease states with reduced GJ coupling. β-AR activation inhibited alternans only after partial GJ uncoupling, and in isolated ventricular myocytes. We infer that normal spatial electrical coupling of myocytes can limit alternans and thereby reduce the ability of β-AR stimulation to suppress alternans.

4.1. Pacing-induced Ca^{2+} alternans in intact hearts follows distinct patterns

CaT and alternans analysis was performed over a range of stimulation frequencies using a formula described before [8, 30]. At 5 Hz only a low percentage of cells displayed alternans, but at 7 Hz virtually all cells exhibited alternans. To ensure large alternans ratios did not result from failed APs, we simultaneously measured $[Ca^{2+}]_i$ with Fluo-8 and V_m with Di-4-

ANEPPS. These data indicate that even at 7 Hz stimulation, every electrical stimulus led to a local AP. At higher rates there might be reduced AP fidelity, but we confined analysis to ≤7 Hz. We believe the alternans seen here is a result of Ca^{2+} refractoriness, in particular RyR refractoriness as previously described [15, 18]. This agrees with the finding that in whole heart optical mapping studies Ca^{2+} alternans with large ratios can be seen even if APD alternans is small [18].

4.2. Reduced GJ coupling alters myocyte alternans and response to β-AR stimulation

β-AR stimulation in isolated cardiac myocytes has been shown to suppress Ca^{2+} alternans [32] and that is also seen in intact rabbit hearts [18]. This is generally attributed to the combination of ISO-induced effects on myocyte Ca^{2+} handling (increased Ca^{2+} current, faster SR Ca^{2+} uptake and consequent shorter RyR restitution) [15, 23–25]. Thus we were quite surprised that in normally coupled hearts ISO failed to reduce the number of alternating cells or alternans amplitude, especially at this alternans threshold range of 5 Hz here. This is not a simple matter of species difference, because we observed that ISO suppressed alternans in both isolated mouse myocytes and partially uncoupled hearts. There are other reports of weak β-AR effects on alternans in the whole heart [32], raising the possibility that strong electrical coupling in the intact heart may limit the ability of ISO to suppress alternans. We do not have a clear mechanistic explanation for this, but it is possible that once alternans is established and stabilized spatially in the well coupled heart, ISO is not as effective in terminating the alternans.

In contrast, the GJ inhibitor CBX increased Ca^{2+} alternans, and restored the expected ability of ISO to suppress alternans. We assume that the CBX effects are primarily via electrical communication between cells (rather than on Ca^{2+}), because Ca^{2+} crosses from cell to cell slowly, Ca^{2+} waves normally cannot propagate from myocyte to myocyte, and high local $[Ca^{2+}]_i$ can reduce GJ conductance [33–35]. In poorly coupled tissue, β-AR stimulation suppressed CaT alternans occurrence and ratio, albeit less completely than in totally uncoupled single myocytes. Cx43 is affected by adenosine receptor stimulation through phosphorylation by PKC leading to its degradation [36] or increase of the GJ closed state [37]. There is evidence that GJ function can be altered by β-AR stimulation in the short term or the long term [38]. Our findings indicate that normal electrical coupling plays a pivotal role in limiting the onset of alternans in the heart, and thus electrical feedback onto local CaT may mediate this effect. Even small local changes in diastolic V_m can influence Ca^{2+} handling such as Ca^{2+} sparks and waves [39].

Gender differences have been described in the capacity to respond to β-AR stimulation, with a reduced effect of β-AR agonists and a reduced arrhythmic activity in females [40]. Interestingly, higher expression levels of Cx43 were found in females compared to males [41], but a direct link has not been proven yet.

Na^+-channels provide the current necessary for the generation of an AP that propagates between cells via GJs, and a reduction of Cx43 expression leads to loss of Na^+-current amplitude [42]. Also cell-cell transfer of charge might also occur through an electric field mechanism [43], highlighting the influence of GJ-conductivity on AP shape.

We found a high degree of synchrony of release between neighboring cells within a field of view and within single cells, but the time-to-peak of the CaT was prolonged upon partial uncoupling. The slowed CaT rise time is most likely because of changes in the local AP shape, because even small changes in AP shape could alter CaTs. Partial GJ uncoupling reduces conduction velocity [44, 45] but does not alter CaT duration [46]. CBX does not alter I_{Ca}, I_{Na} or I_K [44], but can prolong APD in the intact heart [47]. The slower rate of AP rise because of slowed conduction could be responsible for the small slowing of $[Ca^{2+}]_i$ rise, because of slightly less synchronous SR Ca^{2+} release. That would have less effect on $[Ca^{2+}]_i$ decline, in which we did not find significant changes upon CBX addition.

4.3. GJ uncoupling enhances alternans

Partial GJ inhibition did have a strong effect on CaT alternans, significantly increasing the occurrence and intensity. Presumably in this state, weakened electrical communication with other cells allows individual cells to exhibit alternans more readily. The implication is that strong coupling normally suppresses those cells from exhibiting alternans. This may be another manifestation of strong feedback between V_m (which has a long spatial influence) and Ca^{2+} which is more locally regulated. That is, normal V_m coupling may suppress Ca^{2+} alternans, in the same way that when alternans are present, they are almost always spatially concordant (which would not be expected for Ca^{2+} release by itself). Put another way, V_m coupling may cause a smoothing of the Ca^{2+} signal over many cells, both preventing alternans, but also making them spatially concordant when they exist. This behavior is also expected to translate into mechanical alternans, and the feedback from alternans to APD and T-wave alternans that are clinically diagnostic for arrhythmia propensity. Our findings are supported by experiments in ischemic hearts [48] as well as studies on cardiac syncytium [49], where opening of the gap junctions has antiarrhythmic effects.

4.4. Alternans occurs at lower rates with GJ uncoupling and is spatially concordant

Under steady state conditions, we observed only alternans that were in-phase among neighboring myocytes, independent of GJ coupling. We also evaluated the onset of frequency-induced alternans. We found that even after increasing the pacing frequency all cells are synchronized already at the onset of alternans, but that this phase-locking is not dictated by the initially short diastolic interval. Rather phase-locking is driven by electrical coupling, after a short compensated phase where alternans is absent. This is reminiscent of the positive feedback process of Ca^{2+} and voltage that is responsible for regional synchronization of alternans in tissue as described in a mathematical model by Sato et al. [50]. They also found that spatially discordant alternans is Ca^{2+} dependent via interaction with V_m, and can occur over a time course of seconds to minutes.

The brief compensated phase may reflect a period where cells can cope (perhaps energetically) with a higher demand, but at some point RyR refractoriness may initiate alternans. β-AR stimulation (which should have energetic consequences) did not alter the window of compensated Ca^{2+} cycling, so that does not clarify the mechanism. Alternans also depends on stimulation history and site [51]. Conduction velocity (CV) restitution has long been proposed to be an important factor in the development of alternans, and cardiac memory during alternans development can slow APD accommodation [52–54], and thus

delay the onset of CaT alternans. The fact that GJ uncoupling reduced this window of compensated Ca^{2+} handling by two thirds, leads us to infer that intercellular communication may play a pivotal role in this transition behavior with respect to Ca^{2+} cycling pattern (rather than subcellular factors). Reduced GJ coupling alters CV restitution [55] and that might be more impactful at the onset of alternans in poorly coupled tissue.

4.5. Limitations

For the confocal studies presented here, it was crucial to eliminate motion artifacts using blebbistatin, although we are aware that this might prevent mechanical feedback to Ca^{2+} handling and electrophysiology in myocytes [56, 57]. But at least blebbistatin appears not to alter Ca^{2+} handling [58, 59] and we could not find blebbistatin effects [60] in our setup.

We performed our study at room temperature, in part because alternans is more readily induced at lower temperature, but also because the myocytes lose the Ca^{2+} indicator more rapidly at 37°C. Myles et al. [61] have recorded alternans at various temperatures and Pastore et al. [10] studied alternans at both 27 and 37°C and found no mechanistic differences.

Myocytes in culture can electrically couple to fibroblasts and that may have potential pro-arrhythmic effects [62, 63]. Modeling studies have also shown that fibroblast-myocytes coupling can enhance or inhibit alternans [64]. However, we cannot draw conclusions from our experiments here as to any particular role of fibroblast-myocyte coupling in alternans.

4.6. Conclusions

Alternans in tissue is strongly dependent on electrotonic coupling between cells via GJ, and that provides a protective mechanism for cardiac Ca^{2+} instabilities. In contrast to findings in single cells, β-AR stimulation did not curtail alternans in the whole organ with normal GJ coupling, but reduced alternans in partially uncoupled tissue. We hypothesize that electrotonic coupling in the heart normally provides stabilization against alternans, but that β-AR stimulation only limited alternans when coupling was reduced (as occurs under pathological conditions). The initiation of alternans on the organ level does not depend on the preceding diastolic interval per se, but rather on Ca^{2+} instabilities that develop over a defined time course and regional electrical coupling. Taken together, our data suggest that cardiac Ca^{2+} alternans on the tissue level is intimately linked to cell-to-cell electrical coupling via gap-junctions. Thus, GJ uncoupling is critical in developing more severe proarrhythmic events in the heart.

Supplementary Material

Refer to Web version on PubMed Central for supplementary material.

Acknowledgments

We are grateful to Dr. Eckard Picht for helpful suggestions during early phases of this work and Dr. Kenneth Ginsburg for his technical advice. This work was supported by NIH P01-HL080101 and R37-HL030077 (D.M.B.) and FWF T607-B23 (S.L.).

References

1. Diaz ME, O'Neill SC, Eisner DA. Sarcoplasmic reticulum calcium content fluctuation is the key to cardiac alternans. Circ Res. 2004; 94:650–6. [PubMed: 14752033]
2. Tao T, O'Neill SC, Diaz ME, Li YT, Eisner DA, Zhang H. Alternans of cardiac calcium cycling in a cluster of ryanodine receptors: a simulation study. Am J Physiol Heart Circ Physiol. 2008; 295:H598–609. [PubMed: 18515647]
3. Huser J, Wang YG, Sheehan KA, Cifuentes F, Lipsius SL, Blatter LA. Functional coupling between glycolysis and excitation-contraction coupling underlies alternans in cat heart cells. J Physiol. 2000; 524(Pt 3):795–806. [PubMed: 10790159]
4. Diaz ME, Eisner DA, O'Neill SC. Depressed ryanodine receptor activity increases variability and duration of the systolic Ca^{2+} transient in rat ventricular myocytes. Circ Res. 2002; 91:585–93. [PubMed: 12364386]
5. Wan XP, Laurita KR, Pruvot EJ, Rosenbaum DS. Molecular correlates of repolarization alternans in cardiac myocytes. Journal of Molecular and Cellular Cardiology. 2005; 39:419–28. [PubMed: 16026799]
6. Chudin E, Goldhaber J, Garfinkel A, Weiss J, Kogan B. Intracellular Ca^{2+} dynamics and the stability of ventricular tachycardia. Biophysical Journal. 1999; 77:2930–41. [PubMed: 10585917]
7. Qu Z, Nivala M, Weiss JN. Calcium alternans in cardiac myocytes: order from disorder. J Mol Cell Cardiol. 2013; 58:100–9. [PubMed: 23104004]
8. Kockskamper J, Blatter LA. Subcellular Ca^{2+} alternans represents a novel mechanism for the generation of arrhythmogenic Ca^{2+} waves in cat atrial myocytes. J Physiol. 2002; 545:65–79. [PubMed: 12433950]
9. Flore V, Claus P, Symons R, Smith GL, Sipido KR, Willems R. Can body surface microvolt T-wave alternans distinguish concordant and discordant intracardiac alternans? Pacing Clin Electrophysiol. 2013; 36:1007–16. [PubMed: 23614703]
10. Pastore JM, Girouard SD, Laurita KR, Akar FG, Rosenbaum DS. Mechanism linking T-wave alternans to the genesis of cardiac fibrillation. Circulation. 1999; 99:1385–94. [PubMed: 10077525]
11. Aistrup GL, Balke CW, Wasserstrom JA. Arrhythmia triggers in heart failure: the smoking gun of $[Ca^{2+}]_i$ dysregulation. Heart Rhythm. 2011; 8:1804–8. [PubMed: 21699870]
12. Kapur S, Aistrup GL, Sharma R, Kelly JE, Arora R, Zheng J, et al. Early development of intracellular calcium cycling defects in intact hearts of spontaneously hypertensive rats. Am J Physiol Heart Circ Physiol. 2010; 299:H1843–53. [PubMed: 20889840]
13. Verrier RL, Malik M. Electrophysiology of T-wave alternans: mechanisms and pharmacologic influences. J Electrocardiol. 2013; 46:580–4. [PubMed: 23948521]
14. Narayan SM, Bode F, Karasik PL, Franz MR. Alternans of atrial action potentials during atrial flutter as a precursor to atrial fibrillation. Circulation. 2002; 106:1968–73. [PubMed: 12370221]
15. Picht E, DeSantiago J, Blatter LA, Bers DM. Cardiac alternans do not rely on diastolic sarcoplasmic reticulum calcium content fluctuations. Circ Res. 2006; 99:740–8. [PubMed: 16946134]
16. Ramay HR, Liu OZ, Sobie EA. Recovery of cardiac calcium release is controlled by sarcoplasmic reticulum refilling and ryanodine receptor sensitivity. Cardiovasc Res. 2011; 91:598–605. [PubMed: 21613275]
17. Bers, DM. Excitation-Contraction Coupling and Cardiac Contractile Force. 2. Dordrecht, Netherlands: Kluwer Academic Press; 2001.
18. Wang L, Myles RC, De Jesus NM, Ohlendorf AK, Bers DM, Ripplinger CM. Optical Mapping of Sarcoplasmic Reticulum Ca^{2+} in the Intact Heart: Ryanodine Receptor Refractoriness During Alternans and Fibrillation. Circ Res. 2014; 114:1410–21. [PubMed: 24568740]
19. Thimm J, Mechler A, Lin H, Rhee S, Lal R. Calcium-dependent open/closed conformations and interfacial energy maps of reconstituted hemichannels. J Biol Chem. 2005; 280:10646–54. [PubMed: 15615707]
20. Spray DC, White RL, Mazet F, Bennett MV. Regulation of gap junctional conductance. Am J Physiol. 1985; 248:H753–64. [PubMed: 2408489]

21. Rohr S. Role of gap junctions in the propagation of the cardiac action potential. Cardiovasc Res. 2004; 62:309–22. [PubMed: 15094351]
22. Li C, Meng Q, Yu X, Jing X, Xu P, Luo D. Regulatory effect of connexin 43 on basal Ca^{2+} signaling in rat ventricular myocytes. PLoS One. 2012; 7:e36165. [PubMed: 22577485]
23. Bers DM. Cardiac excitation-contraction coupling. Nature. 2002; 415:198–205. [PubMed: 11805843]
24. Eisner D, Bode E, Venetucci L, Trafford A. Calcium flux balance in the heart. J Mol Cell Cardiol. 2013; 58:110–7. [PubMed: 23220128]
25. Ogrodnik J, Niggli E. Increased Ca^{2+} leak and spatiotemporal coherence of Ca^{2+} release in cardiomyocytes during beta-adrenergic stimulation. J Physiol. 2010; 588:225–42. [PubMed: 19900959]
26. Florea SM, Blatter LA. Regulation of cardiac alternans by β-adrenergic signaling pathways. Am J Physiol Heart Circ Physiol. 2012; 303:H1047–56. [PubMed: 22904161]
27. Ljubojevic S, Walther S, Asgarzoei M, Sedej S, Pieske B, Kockskamper J. In situ calibration of nucleoplasmic versus cytoplasmic Ca^{2+} concentration in adult cardiomyocytes. Biophys J. 2011; 100:2356–66. [PubMed: 21575569]
28. Euler DE. Cardiac alternans: mechanisms and pathophysiological significance. Cardiovasc Res. 1999; 42:583–90. [PubMed: 10533597]
29. Aistrup GL, Kelly JE, Kapur S, Kowalczyk M, Sysman-Wolpin I, Kadish AH, et al. Pacing-induced heterogeneities in intracellular Ca^{2+} signaling, cardiac alternans, and ventricular arrhythmias in intact rat heart. Circ Res. 2006; 99:e65–73. [PubMed: 16960102]
30. Wu Y, Clusin WT. Calcium transient alternans in blood-perfused ischemic hearts: observations with fluorescent indicator fura red. Am J Physiol. 1997; 273:H2161–9. [PubMed: 9374749]
31. Shy D, Gillet L, Ogrodnik J, Albesa M, Verkerk AO, Wolswinkel R, et al. PDZ domain-binding motif regulates cardiomyocyte compartment-specific NaV1.5 channel expression and function. Circulation. 2014; 130:147–60. [PubMed: 24895455]
32. Ng GA, Brack KE, Patel VH, Coote JH. Autonomic modulation of electrical restitution, alternans and ventricular fibrillation initiation in the isolated heart. Cardiovasc Res. 2007; 73:750–60. [PubMed: 17217937]
33. Rudisuli A, Weingart R. Electrical properties of gap junction channels in guinea-pig ventricular cell pairs revealed by exposure to heptanol. Pflugers Arch. 1989; 415:12–21. [PubMed: 2482959]
34. Maurer P, Weingart R. Cell pairs isolated from adult guinea pig and rat hearts: effects of $[Ca^{2+}]_i$ on nexal membrane resistance. Pflugers Arch. 1987; 409:394–402. [PubMed: 3627957]
35. Wier WG, ter Keurs HE, Marban E, Gao WD, Balke CW. Ca^{2+} 'sparks' and waves in intact ventricular muscle resolved by confocal imaging. Circ Res. 1997; 81:462–9. [PubMed: 9314826]
36. Popolo A, Morello S, Sorrentino R, Pinto A. Antiadrenergic effect of adenosine involves connexin 43 turn-over in H9c2 cells. Eur J Pharmacol. 2013; 715:56–61. [PubMed: 23834776]
37. Johnstone SR, Billaud M, Lohman AW, Taddeo EP, Isakson BE. Posttranslational modifications in connexins and pannexins. J Membr Biol. 2012; 245:319–32. [PubMed: 22739962]
38. Campbell AS, Johnstone SR, Baillie GS, Smith G. β-Adrenergic modulation of myocardial conduction velocity: Connexins vs. sodium current. J Mol Cell Cardiol. 2014; 77C:147–54. [PubMed: 25453599]
39. Sato D, Bartos DC, Ginsburg KS, Bers DM. Depolarization of cardiac membrane potential synchronizes calcium sparks and waves in tissue. Biophysical Journal. 2014 In Press.
40. Hoeker GS, Hood AR, Katra RP, Poelzing S, Pogwizd SM. Sex differences in β-adrenergic responsiveness of action potentials and intracellular calcium handling in isolated rabbit hearts. PLoS One. 2014; 9:e111411. [PubMed: 25340795]
41. Stauffer BL, Sobus RD, Sucharov CC. Sex differences in cardiomyocyte connexin43 expression. J Cardiovasc Pharmacol. 2011; 58:32–9. [PubMed: 21753256]
42. Jansen JA, Noorman M, Musa H, Stein M, de Jong S, van der Nagel R, et al. Reduced heterogeneous expression of Cx43 results in decreased Nav1.5 expression and reduced sodium current that accounts for arrhythmia vulnerability in conditional Cx43 knockout mice. Heart Rhythm. 2012; 9:600–7. [PubMed: 22100711]

43. Agullo-Pascual E, Delmar M. The noncanonical functions of Cx43 in the heart. J Membr Biol. 2012; 245:477–82. [PubMed: 22825715]
44. de Groot JR, Veenstra T, Verkerk AO, Wilders R, Smits JP, Wilms-Schopman FJ, et al. Conduction slowing by the gap junctional uncoupler carbenoxolone. Cardiovasc Res. 2003; 60:288–97. [PubMed: 14613858]
45. Kojodjojo P, Kanagaratnam P, Segal OR, Hussain W, Peters NS. The effects of carbenoxolone on human myocardial conduction: a tool to investigate the role of gap junctional uncoupling in human arrhythmogenesis. J Am Coll Cardiol. 2006; 48:1242–9. [PubMed: 16979013]
46. Myles RC, Wang L, Kang C, Bers DM, Ripplinger CM. Local β-adrenergic stimulation overcomes source-sink mismatch to generate focal arrhythmia. Circ Res. 2012; 110:1454–64. [PubMed: 22539768]
47. Howarth FC, Qureshi MA. Effects of carbenoxolone on heart rhythm, contractility and intracellular calcium in streptozotocin-induced diabetic rat. Mol Cell Biochem. 2006; 289:21–9. [PubMed: 16583133]
48. Kjolbye AL, Dikshteyn M, Eloff BC, Deschenes I, Rosenbaum DS. Maintenance of intercellular coupling by the antiarrhythmic peptide rotigaptide suppresses arrhythmogenic discordant alternans. Am J Physiol Heart Circ Physiol. 2008; 294:H41–9. [PubMed: 17982010]
49. Jia Z, Bien H, Shiferaw Y, Entcheva E. Cardiac cellular coupling and the spread of early instabilities in intracellular Ca^{2+} Biophys J. 2012; 102:1294–302. [PubMed: 22455912]
50. Sato D, Bers DM, Shiferaw Y. Formation of spatially discordant alternans due to fluctuations and diffusion of calcium. PLoS One. 2013; 8:e85365. [PubMed: 24392005]
51. Gizzi A, Cherry EM, Gilmour RF Jr, Luther S, Filippi S, Fenton FH. Effects of pacing site and stimulation history on alternans dynamics and the development of complex spatiotemporal patterns in cardiac tissue. Front Physiol. 2013; 4:71. [PubMed: 23637684]
52. Watanabe MA, Koller ML. Mathematical analysis of dynamics of cardiac memory and accommodation: theory and experiment. Am J Physiol Heart Circ Physiol. 2002; 282:H1534–47. [PubMed: 11893591]
53. Kalb SS, Dobrovolny HM, Tolkacheva EG, Idriss SF, Krassowska W, Gauthier DJ. The restitution portrait: a new method for investigating rate-dependent restitution. J Cardiovasc Electrophysiol. 2004; 15:698–709. [PubMed: 15175067]
54. Mironov S, Jalife J, Tolkacheva EG. Role of conduction velocity restitution and short-term memory in the development of action potential duration alternans in isolated rabbit hearts. Circulation. 2008; 118:17–25. [PubMed: 18559701]
55. Stein M, van Veen TA, Hauer RN, de Bakker JM, van Rijen HV. A 50% reduction of excitability but not of intercellular coupling affects conduction velocity restitution and activation delay in the mouse heart. PLoS One. 2011; 6:e20310. [PubMed: 21673812]
56. Prosser BL, Ward CW, Lederer WJ. X-ROS signaling: rapid mechano-chemo transduction in heart. Science. 2011; 333:1440–5. [PubMed: 21903813]
57. Jian Z, Han H, Zhang T, Puglisi J, Izu LT, Shaw JA, et al. Mechanochemotransduction during cardiomyocyte contraction is mediated by localized nitric oxide signaling. Sci Signal. 2014; 7:ra27. [PubMed: 24643800]
58. Fedorov VV, Lozinsky IT, Sosunov EA, Anyukhovsky EP, Rosen MR, Balke CW, et al. Application of blebbistatin as an excitation-contraction uncoupler for electrophysiologic study of rat and rabbit hearts. Heart Rhythm. 2007; 4:619–26. [PubMed: 17467631]
59. Lou Q, Li W, Efimov IR. The role of dynamic instability and wavelength in arrhythmia maintenance as revealed by panoramic imaging with blebbistatin vs. 2,3-butanedione monoxime. Am J Physiol Heart Circ Physiol. 2012; 302:H262–9. [PubMed: 22037192]
60. Brack KE, Narang R, Winter J, Ng GA. The mechanical uncoupler blebbistatin is associated with significant electrophysiological effects in the isolated rabbit heart. Exp Physiol. 2013; 98:1009–27. [PubMed: 23291912]
61. Myles RC, Burton FL, Cobbe SM, Smith GL. Alternans of action potential duration and amplitude in rabbits with left ventricular dysfunction following myocardial infarction. J Mol Cell Cardiol. 2011; 50:510–21. [PubMed: 21145895]

62. Miragoli M, Gaudesius G, Rohr S. Electrotonic modulation of cardiac impulse conduction by myofibroblasts. Circ Res. 2006; 98:801–10. [PubMed: 16484613]

63. Zlochiver S, Munoz V, Vikstrom KL, Taffet SM, Berenfeld O, Jalife J. Electrotonic myofibroblast-to-myocyte coupling increases propensity to reentrant arrhythmias in two-dimensional cardiac monolayers. Biophys J. 2008; 95:4469–80. [PubMed: 18658226]

64. Xie Y, Garfinkel A, Weiss JN, Qu Z. Cardiac alternans induced by fibroblast-myocyte coupling: mechanistic insights from computational models. Am J Physiol Heart Circ Physiol. 2009; 297:H775–84. [PubMed: 19482965]

Highlights

- Ca^{2+} alternans were measured via confocal imaging of neighboring myocytes within the whole heart.
- These local alternans were virtually always concordant (in-phase) among neighboring myocytes, independent of the diastolic interval prior to alternans initiation.
- Partial gap junction uncoupling increased the propensity for alternans, and made alternans more susceptible to suppression by β-adrenergic activation.
- Cell-cell electrical communication appears to be essential in synchronizing the phase of alternans among neighboring myocytes in the whole heart.

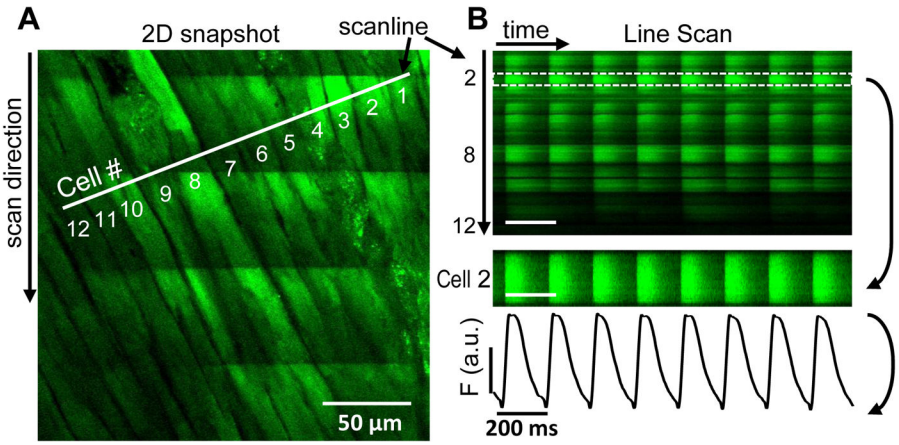

Figure 1. Confocal Ca^{2+} in single myocytes within intact heart

Two-dimensional image of observed area on left ventricular (LV) surface recorded with a point scanning confocal microscope shows position of selected scan line on the epicardial LV surface (**A**). During image acquisition several Ca^{2+} transients are visible as increased fluorescence from top to bottom (as time elapses). The scan line image is used to analyze Ca^{2+} transients in individual single cells (**B**).

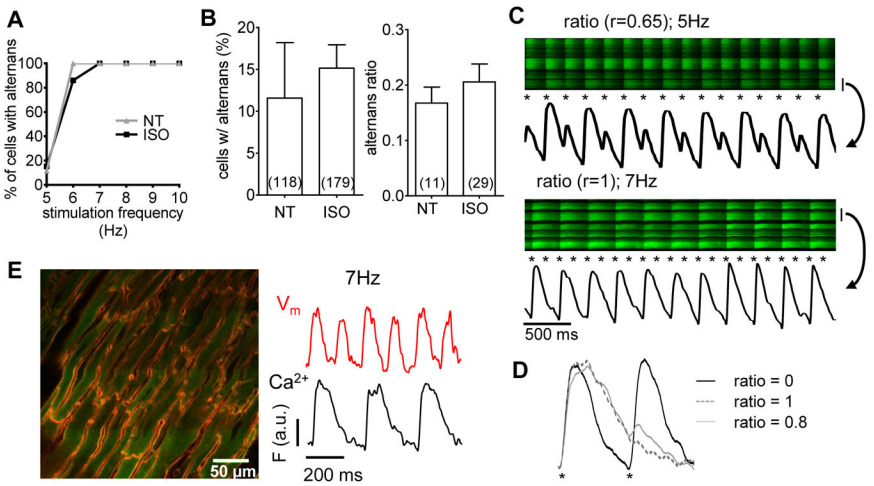

Figure 2. Pacing induced Ca^{2+} alternans

Langendorff-perfused mouse hearts under control conditions (NT) or under β-AR stimulation (ISO) were electrically stimulated at increasing frequencies and percentage of cells exhibiting alternans was assessed (**A**). At 5 Hz the percentage of cells with alternans and alternans ratio were unaffected by β-AR stimulation (**B**). Two examples of high alternans ratio are displayed. The bar at right of image indicates the cell from which signals were taken and the asterisks indicate stimuli (**C**). Representative transients from tissue stimulated at 5 Hz are displayed for no alternans (ratio = 0), maximal alternans (ratio = 1) and substantial alternans (r= 0.8; **D**). 2D image of a heart loaded with both with Ca^{2+} and voltage sensor (**E**, left). Correspondence of voltage (V_m) with Ca^{2+} from the same cell during 6 stimulated beats confirms action potential occurrence at missing Ca^{2+} transients (for r=1; **E**).

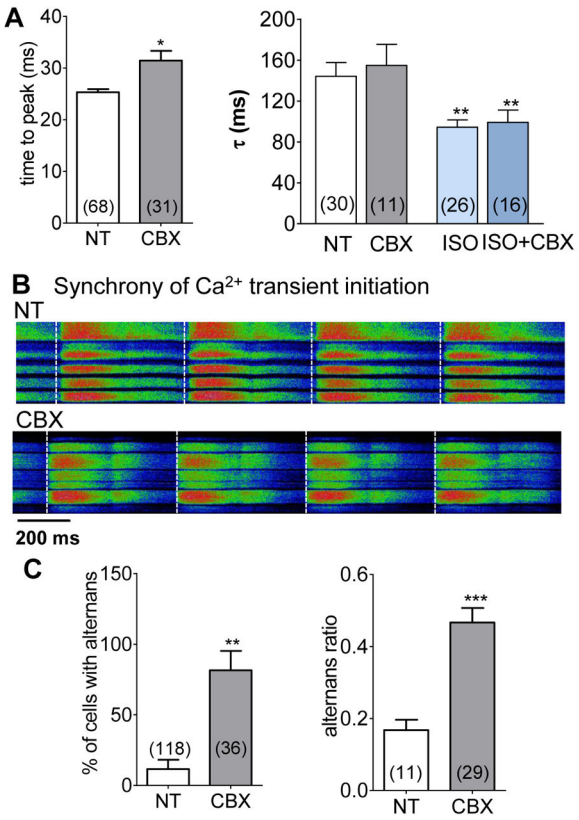

Figure 3. Ca^{2+} release with partial electrical uncoupling

Partial GJ uncoupling slightly prolongs Ca^{2+} transient time to peak, but not [Ca^{2+}] decline (**A**). Initiation of CaT among neighboring cells is synchronous in NT and with CBX (dashed lines; **B**). Alternans incidence and amplitude are increased by partial GJ uncoupling (**C**).

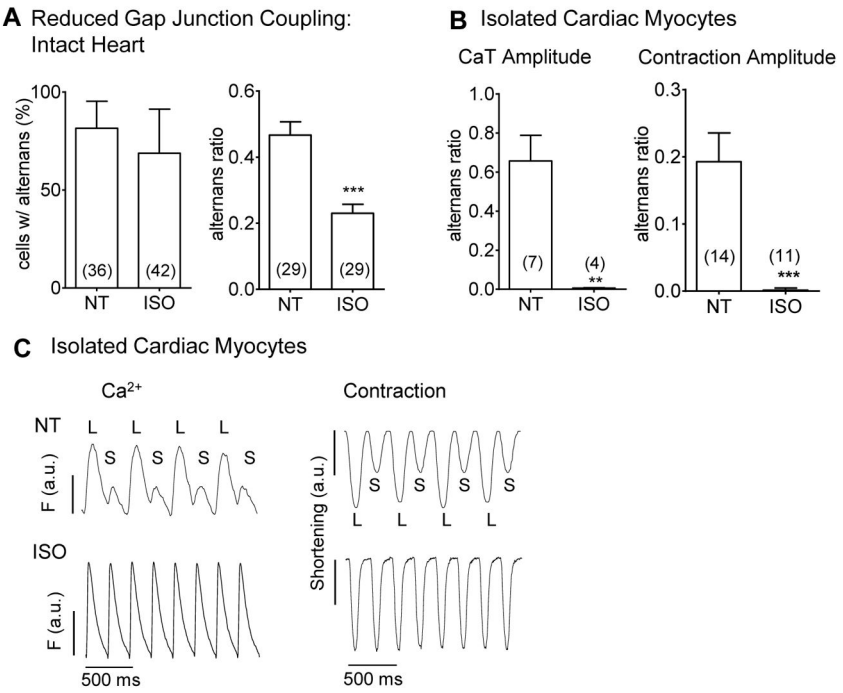

Figure 4. β-AR activation limits alternans amplitude during reduced GJ coupling

In intact heart with partial GJ uncoupling (25 μM CBX) β-AR agonist ISO reduces alternans amplitude, but not incidence (**A**). In isolated myocytes stimulated at 5 Hz, ISO abolished Ca^{2+} and contractile alternans (**B**). Exemplar traces from myocytes stimulated at 5Hz in NT (±ISO) for Ca^{2+} (left) and contraction (right, **C**).

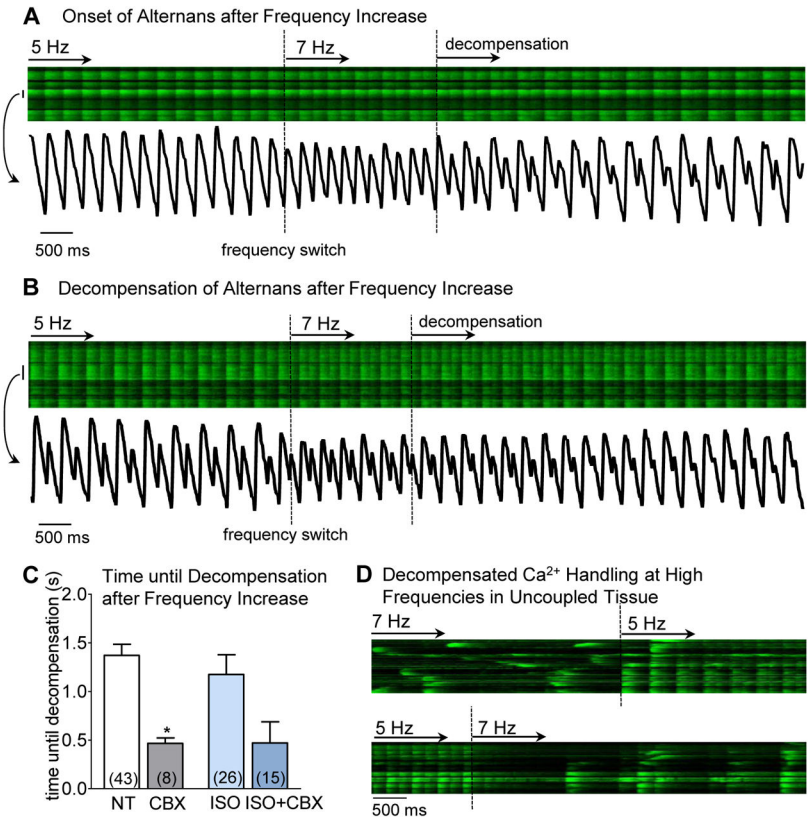

Figure 5. Transition from normal Ca^{2+} cycling to stable alternans

An example of tissue in ISO during increase in stimulation frequency from 5 to 7 Hz with intensity plot for the cell marked with a bar (**A**). Dashed lines indicate frequency change and transition to decompensated Ca^{2+} handling (alternans). **B** another example where alternans was already present at 5 Hz (r = 0.454) and upon frequency increase (first dashed line) the ratio was slightly reduced to r = 0.417, but then increased to r= 0.55 and 0.85 after decompensation (at second dashed line). Time frame until decompensation was reduced by GJ uncoupling in NT and ISO similarly (**C**). During β-AR stimulation some episodes of decompensated Ca^{2+} handling were observed where cells only recovered upon frequency decrease (**D**).

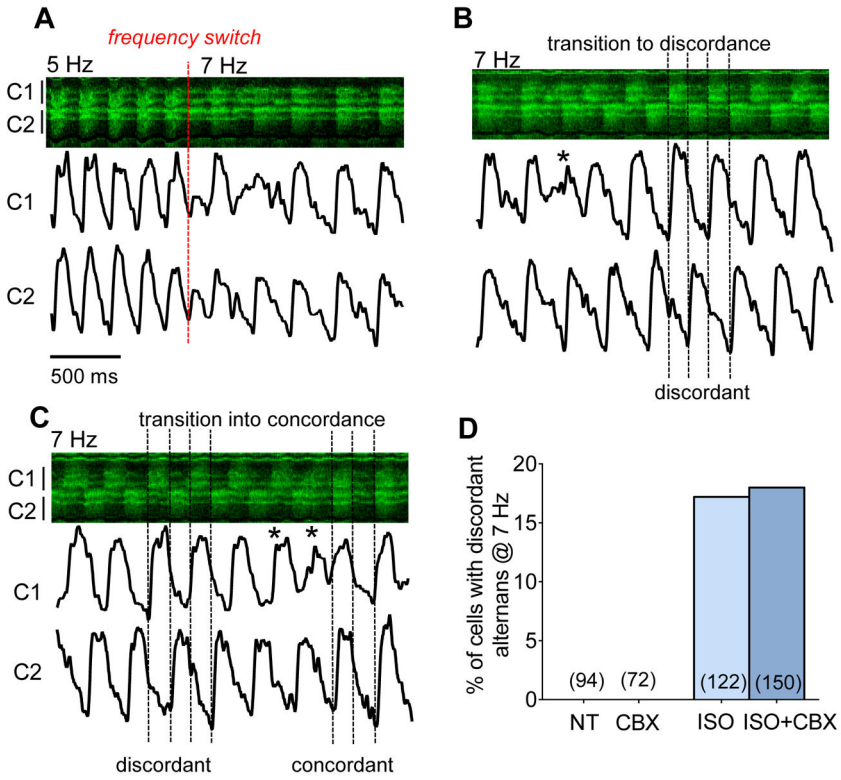

Figure 6. Transition from spatially discordant to concordant behavior

Exemplar recording in ISO with a frequency increase from 5 to 7 Hz, showing 3 phases (**A–C**) with intensity profiles of two neighboring cells. The first beat at shorter BCL is reduced and quickly transitions to concordant alternans (**A**), which devolves into discordant alternans (**B**) before reverting (*) to stable concordant alternans (**C**). Spatially discordance was only observed in a subset of β-AR stimulated hearts and was independent of partial GJ uncoupling (**D**).